IMMERSED BOUNDARY PENALTY METHOD
FOR COMPRESSIBLE FLOWS OVER MOVING OBSTACLES

ILYA ABALAKIN, NATALIA ZHDANOVA AND TATIANA KOZUBSKAYA

Keldysh Institute of Applied Mathematics,
4A, Miusskaya Sq., Moscow, 125047, Russia
nat.zhdanova@gmail.com, http://caa.imamod.ru/

Key words: Unstructured Mesh, Immersed Boundary Method, Edge-Based Scheme, Fluid-Structure Interaction, Moving Body, Compressible Flow

Abstract. A non-boundary conforming method for numerical simulation of compressible flows over moving obstacles on unstructured meshes is presented. The Brinkman penalization method is used to satisfy the boundary condition on the fluid-structure interface. It allows to consider the problem in simply connected domains and to keep the same higher-accuracy edge-based scheme everywhere including the regions around moving obstacles. The method is applied to simulate forced and induced oscillations of two-dimensional cylinder and flow over pitching and plunging NACA0012 foil. The numerical results are compared with the available experimental data.

1 INTRODUCTION

Fluid-structure interaction processes are an exciting and rapidly growing research field because of the wide range of applicability in different technological areas. This research direction gained much attention from scientists and engineers over the past decades. Nowadays there are various approaches to numerical simulation of flow interaction with moving structures. New engineering challenges require their further development and improvement, which becomes more feasible thanks the rapid growth of performance of modern supercomputers.

Some of these methods are based on analytical and semi-empirical models [1, 2]. Another wide class of methods uses the body-fitted meshes and commonly operates in moving reference frames or involves coordinate transformations [3, 4]. This approach presents a significant difficulty for complex geometries of fluid-structure interfaces and especially for systems of bodies that are prone to large motions and deformations.

Among the non-boundary conforming approaches the immersed boundary methods pioneered by Peskin seem more attractive to handle moving bodies of complex geometries [5,6]. Within this approach the body position and its movement over a computational domain are controlled by an external force field that is prescribed by time-dependent source terms in the governing equations. Further we refer to this method as IBC (immersed boundary condition).

In the present work we use an IBC method, namely the Brinkman penalization method, to mimic the no-slip boundary conditions on the interface between a moving body and compressible viscous fluid. The method is developed for unstructured meshes. Its main

advantage with respect to other immersed boundary penalty methods consists in controlling the boundary approximation error through the value of penalization parameter [7].

The immersed boundary penalty techniques are widely used for incompressible flow simulations [7], [8]. In particular, it has been proved that the solution of the penalized Navier-Stokes equations for incompressible flow converge to the one of the original Navier-Stokes problem while the penalization parameter goes to zero [9]. The papers [10, 11] applied the IBC approach to simulating compressible flows, however the problems under consideration concerned immovable or uniformly moving bodies.

Within the presented approach, the immersed boundary method is used for simulating fluid-structure interaction phenomena on unstructured meshes. It is applied for bodies moving under external or vortex-induced forces. Although the 2D formulations are considered, the algorithm can be naturally extended to 3D cases.

A special attention is paid to predicting the forces acting on the obstacles since the provision of sufficient accuracy at the solid-fluid interfaces is the most challenging problem for the immersed boundary methods.

The developed approach is implemented in the in-house code NOISEtte [12]. The numerical algorithm is built basing on the higher-accuracy edge-based schemes [13] and the second order implicit Newton-based method for the time integration.

2 COMPUTATIONAL APPROACH

For calculating the aerodynamic characteristics of the body, moving under the action of external or induced aerodynamic forces, we use the following mathematical model:
- flow of a viscous compressible fluid is governed by the Navier-Stokes system;
- motion of a rigid body under the action of external or induced aerodynamic forces is modeled by the harmonic oscillator equation.

At the interface between the two media (solid Ω_B and fluid Ω_f), the no-slip condition is imposed:

$$\mathbf{u}\big|_{\partial\Omega_B} = \mathbf{V} \tag{1}$$

where $\mathbf{V}$ is the velocity of the mass center of the body and $\mathbf{u}$ is the velocity of the fluid. The boundary condition (1) is provided by the Brinkman penalization method, which doesn't require explicit matching of the mesh nodes to the solid boundary. To this end, special penalty functions are added to the Navier-Stokes system. These functions differ from zero only at the nodes of the computational grid that lie in the region $\overline{\Omega}_B = \Omega_B \cup \partial\Omega_B$ (inside and on the solid boundary). The Navier-Stokes system with Brinkman penalty terms is

$$\begin{cases} \dfrac{\partial \rho}{\partial t} + \dfrac{\partial \rho u_i}{\partial x_i} = 0 \\[2mm] \dfrac{\partial \rho u_i}{\partial t} + \dfrac{\partial \rho u_i u_j}{\partial x_j} + \dfrac{\partial p_i}{\partial x_i} = \dfrac{\partial \mu \tau_{ij}}{\partial x_j} - \dfrac{\chi}{\eta}\rho\left(u_i - u_{Bi}\right) \\[2mm] \dfrac{\partial E}{\partial t} + \dfrac{\partial \left(E + p\right)u_i}{\partial x_i} = \dfrac{\partial u_j \mu \tau_{ij}}{\partial x_i} + \dfrac{\partial q_i}{\partial x_i} - \dfrac{\chi}{\eta}\rho u_i\left(u_i - u_{Bi}\right). \end{cases} \tag{2}$$

2

The last terms in the momentum and energy equations determine the penalty, where the function χ defines the geometry of a solid at each moment:

$$\chi(t) = \begin{cases} 1, & \mathbf{x} \in \overline{\Omega}_B(t) \\ 0, & \mathbf{x} \in \Omega_f(t). \end{cases}$$

The parameter $\eta \ll 1$ determines the rate of relaxation of the flow velocity to the velocity of the moving body. The value of the penalization parameter 10^{-4} is used for all simulations in this paper.

The numerical solution of system (2) is based on the following approaches. The convective fluxes are approximated using a scheme based on the quasi-one-dimensional reconstruction of the variables along a grid edge (EBR scheme, see [13], [14], [15]). The spatial discretization is based on the vertex-centered formulation, which means that all the unknown variables are determined at nodes surrounded by computation cells (dual mesh).

The viscous terms in the Navier–Stokes system are approximated using the finite-element method with linear basis functions (P1 Galerkin).

The time integration is performed using an implicit second-order scheme followed by the Newtonian linearization of the space-discretized system of equations. At each Newtonian iteration stage the corresponding system of linear equations is solved by Biconjugate gradient stabilized method.

The motion of a solid body with one degree of freedom (in-line motion) exposed to excitations by a fluid flow, is described by the harmonic oscillator equation

$$m\ddot{y} + 2m\zeta\omega\,\dot{y} + k\,y = F_y \tag{3}$$

where y is the displacement, m is the structure mass per unit length, ζ is the damping coefficient of the structure, ω is the circular natural frequency of the structure without fluid surrounding it and k the stiffness parameter. The force F_y denotes the force per unit length exerted on this body. This force is the sum of the inertial force F_I and drag force F_D. The inertial force is due to the fluid acceleration, and the drag force is associated with relative velocity. For a wide class of oscillating flows the force F_y can be represented by the Morison equation [16], [17]

$$F_y^M = \rho A \dot{U} + c_a \rho A (\dot{U} - \ddot{y}) + \frac{1}{2}\rho |U - \dot{y}|(U - \dot{y}) D c_d. \tag{4}$$

Here ρ denotes the fluid density, A the cross-sectional area, U the excitation velocity, and D is a characteristic length of the structure. Two force parameters are included in this equation, the drag coefficient c_d and the added-mass coefficient c_a. The first two terms on the RHS of (4) correspond to the inertial force, and the third one gives the drag. Further equation (4) is used to verify the computational results.

In this paper the two types of solid motion in fluid are considered:

1) the body motion is prescribed according to $\mathbf{x} = \mathbf{G}(t)$;

2) the law of motion is determined by equation (4).

For problems of the first type to advance from the n-th time step to the $(n+1)$-th time step the following algorithm are used:

- computation of the coordinate and velocity of the mass center at time t^{n+1}:

$$\mathbf{x}^{n+1} = \mathbf{G}\left(t^{n+1}\right), \quad \mathbf{u}_B^{n+1} = \frac{d\mathbf{G}}{dt}\left(t^{n+1}\right);$$

- finding the new position of the solid boundary;
- solving system (2) by the fully implicit scheme and calculating variables for time t^{n+1}.

For problems of the second type the modified Navier-Stokes system (2) and the body motion equation (3) are jointly solved:

- computation of the coordinates and velocity of the mass center at time t^{n+1} by the explicit first-order scheme: $\mathbf{u}_B^{n+1} = \mathbf{u}_B^n - \dfrac{\Delta t}{m}\left(F_y^n - 2\zeta\omega\mathbf{u}_B^n - k\,y^n\right)$, $y^{n+1} = y^n - \Delta t\,\mathbf{u}_B^{n+1}$;

- finding the new position of the solid boundary;
- solving system (2) by the fully implicit scheme and calculating variables for time t^{n+1}.

According to the papers [7] и [10], by the asymptotic expansion with respect to the small parameter η, the force of body excitation by the fluid is expressed as

$$\mathbf{F} = -\oint_{\partial\Omega_B}\left(p\,\mathbf{n}_B - \mathbf{S}\cdot\mathbf{n}_B\right)dS = \int_{\Omega_B}\frac{\partial\rho\mathbf{u}_B}{\partial t}dV + \int_{\Omega_B}\nabla\cdot\left(\rho\mathbf{u}_B\otimes\mathbf{u}_B\right)dV + \frac{1}{\eta}\int_{\Omega_B}\rho\left(\mathbf{u}_\eta - \mathbf{u}_B\right)dV. \quad (5)$$

Formula (6) is a generalization for the variable velocity $\mathbf{u}_B$ of the formula obtained in [10] for the constant velocity.

The proposed method is applied to simulation of the test problems initially formulated for incompressible flows. The mean pressure (in the dimensionless variables) $p = 1/\left(\gamma M^2\right)$ is found from the equation of state for the ideal compressible fluid. The Mach number is small, $M = 0.05$, which guarantees that the deviation of density from the mean value is also small, $\rho = 1 + O\left(M^2\right)$, which approximates the conditions in an incompressible flow.

3 RESULTS AND DISCUSSION

3.1 Forced vibrations of a cylinder

The interaction of an oscillating circular cylinder with a quiescent fluid is considered. The position of the mass centre is determined by the simple harmonic oscillation $y(t) = -A\sin\left(2\pi f\,t\right)$. There are two parameters in the problem: $\mathrm{Re} = U_{\max}D/\nu = 100$ – the Reynolds number and $\mathrm{K_c} = U_{\max}/D\,f = 5$ – the Keulegan-Carpenter number. Here D is the cylinder diameter, $U_{\max}$ is the maximum velocity of the cylinder motion and f is the frequency of imposed replacement. Taking the maximum velocity and cylinder diameter as characteristic quantities, the dimensionless frequency and displacement amplitude are defined as $f = 1/K_c = 0.2$ and $A = 1/\left(2\pi f\right)$, correspondingly.
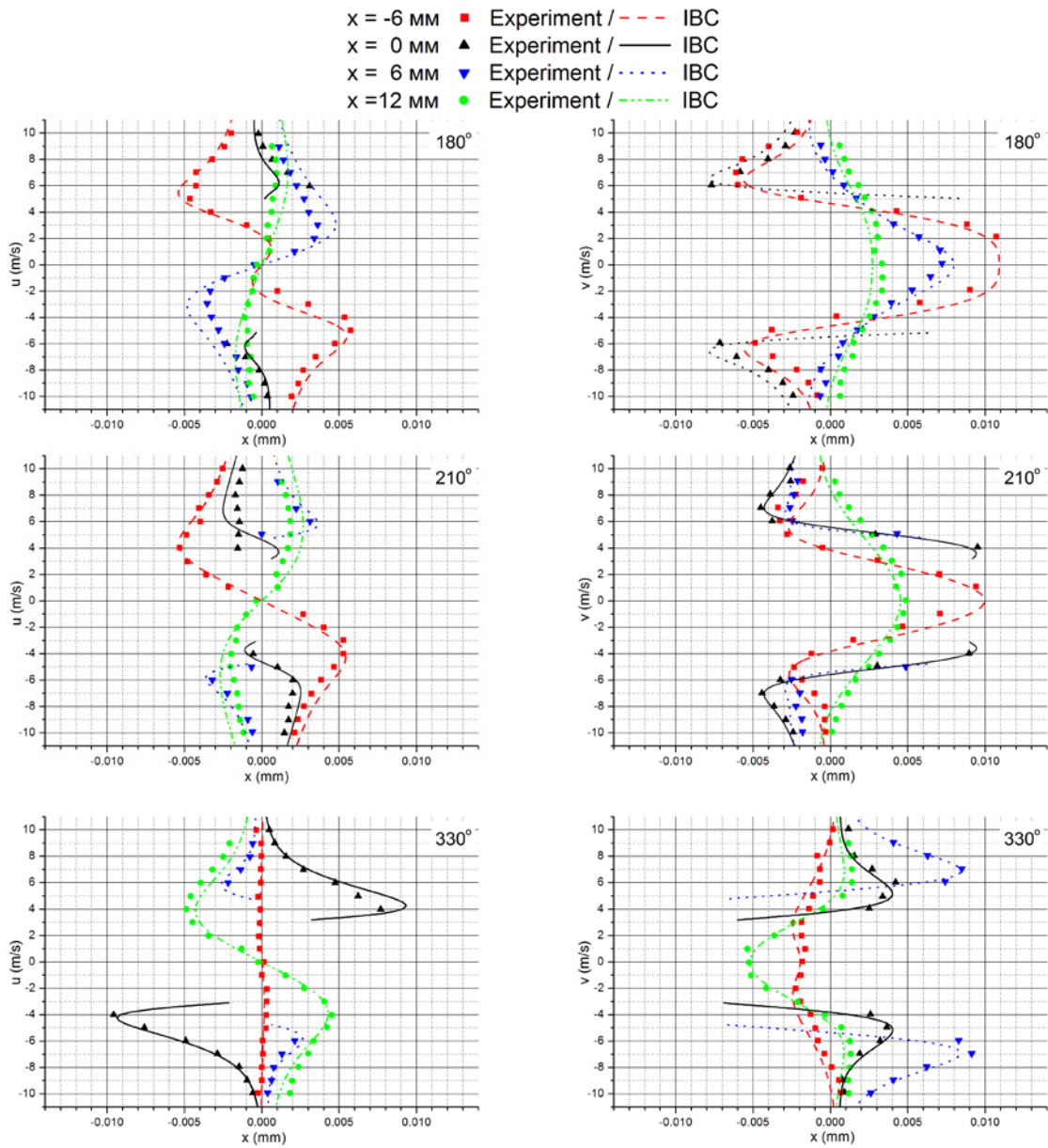
Figure 1: Velocity profiles for different phase angles: $180°$, $210°$ and $330°$

The computational domain is $[-10.0, 15.0] \times [-10.0, 10.0]$. Two different meshes with characteristic cell sizes $\Delta h = 0.02$ and $\Delta h = 0.004$ (coarse and fine meshes) are used.

In Figure 1 the velocity profiles at four locations along x-axis for different phase angles are shown. In general the results agree with experimental data from [18], the same discrepancy is observed in the results of numerical simulation using accelerated reference frames moving with the body [18].

The computed instant in-line force variation is shown in Figure 2 on coarse and fine meshes (IBC method). These results are compared with the result of simulation on body-fitted mesh in the moving reference frame (BF method). Computations using IBC and BF methods

are performed with the same numerical scheme.
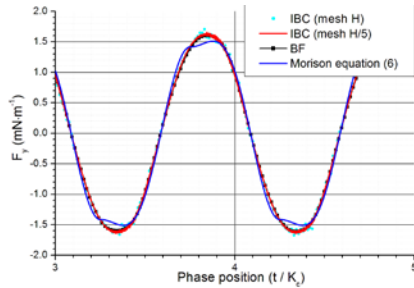
Figure 2: In-line force computed on different mesh

Table 1: Comparison of drag and added mass coefficients for forced vibrations of the cylinder

	c_d	c_a
Fine mesh	2.043	1.433
Coarse mesh	2.036	1.440
Dütsch, 1998	2.09	1.45

Applying dimensionless equation (4) to the oscillatory motion of a circular cylinder in a quiescent fluid, the in-line force $F_y(t)$ acting on the cylinder can be expressed as

$$F_y^M(t) = -\frac{1}{2} c_d \dot{y}(t) |\dot{y}(t)| - \frac{\pi}{4} c_a \ddot{y}(t). \tag{6}$$

Substituting the computed force F_y into equation (6), motion-averaged coefficients c_d and c_a are found using the least-squares method. Computed values of c_d and c_a presented in Table 1 are slightly dependent on the mesh size and in a good agreement with results from [18].

The in-line force $F_y^M(t)$ calculated using equation (6) and the values of c_d and c_a from Table 1 are shown in Figure 2. As seen from the figure the force value provided by the numerical simulation even on the coarse mesh is better than predicted by equation (6).
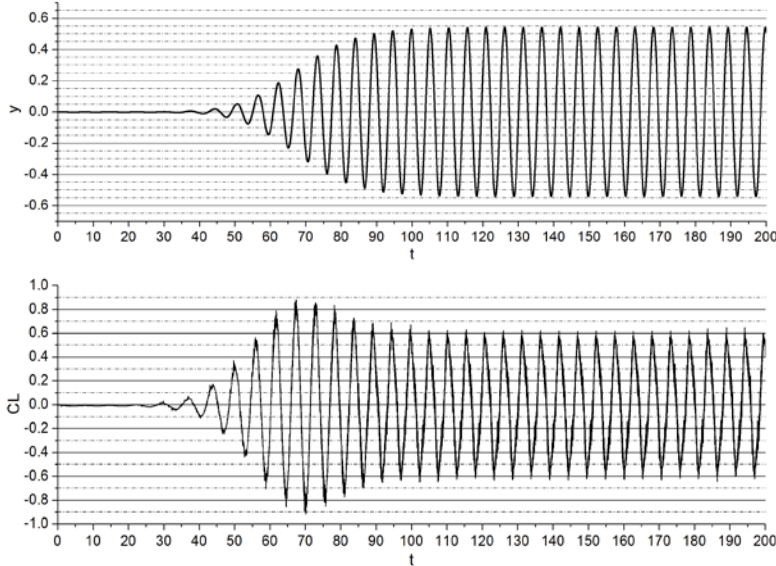
3.2 Vortex-induced vibrations of a cylinder

A two-dimensional cylinder has one degree of freedom and is allowed to move only in the cross-stream direction. The uniform external flow with velocity U_{flow} is imposed in x-direction. The Reynolds number is set to $\mathrm{Re} = U_{flow} D / \nu = 100$. The cylinder is free to move in y-direction from the beginning of integration in time. The computation is continued until a periodic state of constant maximum amplitude is reached.

The movement is induced by the lifting force generated by the flow and is modelled as a forced oscillator (4), where $m = 5$, $\zeta = 0$, $k = 8.74$ and F_y is the flow force evaluated using (5). These values of parameters m, b, k are chosen to compare the computational results with calculations from [2] where numerical simulations were done by viscous-vortex method.

In Figure 3 the computed lift coefficient and replacement of a cylinder are shown. The cylinder oscillates in phase with the lift force and the maximum value of replacement is approximately equal to half of its radius. This agrees with the results obtained in [19]. The lift coefficient is calculated using the force components defined by the vorticity in the boundary layer and wake and doesn't include the inertial component due to the structure acceleration (added mass force).

6

The computed values of replacement amplitude A, lift force amplitude $(C_L)_{rms}$, mean drag value $\bar{C}_D$ and Strouhal number are in a good agreement with the numerical results from [2], as seen from Table 2.

Table 2: Comparison of results for vortex-induced cylinder vibrations

|	Present study	D.Shiels, 2001
A	0.55	0.57
$(C_L)_{rms}$	0.6	0.5
$\bar{C}_D$	2.17	2.26
St	0.2	0.194

Figure 3: Lift coefficient for a vortex-induced cylinder vibrations (top) and cylinder displacement (bottom) as a function of time

3.3 Pitching and plunging airfoil

To verify the method for a more complicated structure geometry and motion law the flow over flapping foil is computed. The result is analyzed in terms of time-averaged and time-dependent aerodynamic loads.

A NACA0012 foil, with the chord length $c = 1$, oscillates with plunging and pitching mechanisms as shown in Figure 4-a. Here the replacement $h(t) = h_0 \sin(\omega t)$ corresponds to the vertical plunging motion with amplitude h_0 and linear frequency $f = \omega/2\pi$. The foil pitches around one-third chord with pitch angle defined as $\theta(t) = \theta_0 \sin(\omega t + \psi)$, where θ_0 denotes the pitch amplitude and ψ is the phase angle between the pitching and plunging motion.

Following an experimental test case by Anderson et al. [20] the plunging amplitude h_0 is set to 0.75, phase angle ψ is set to $\pi/2$ and the Reynolds number is set to $\rho U_{flow} c/\mu = 40\,000$. The computations were carried out for different values of the Strouhal number: 0.25, 0.35, 0.45. For $\psi = \pi/2$ the pitching amplitude θ_0 is expressed as $\theta_0 = \arctan(\pi St) - \alpha_0$ where α_0 is a nominal angle of attack which is set to $15°$.
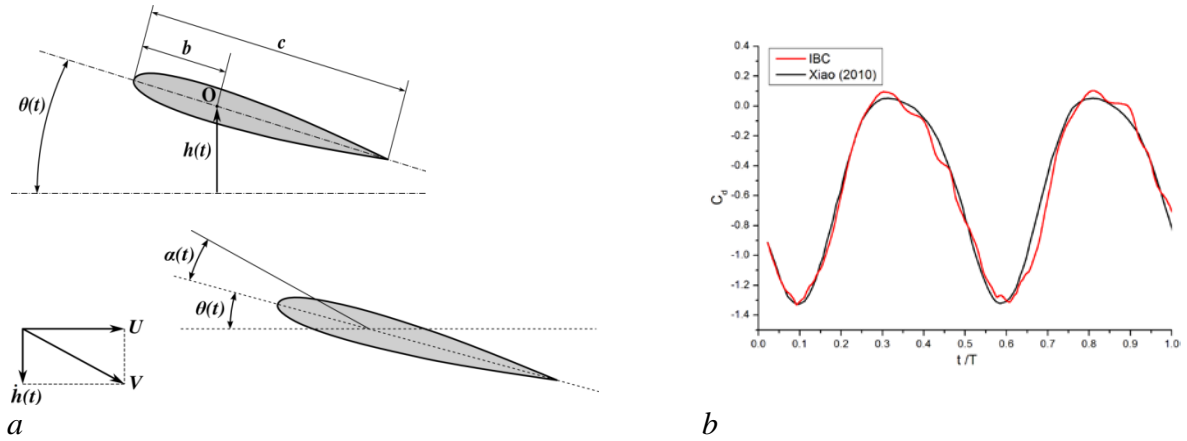
Figure 4: (a) Scheme of the foil pitching and plunging oscillation. (b) Instant drag coefficient

The instant drag coefficient in one period of oscillations with the Strouhal number fixed at $St = 0.35$ correlates with the results of [21] where moving reference frame method is used (Figure 5a). The discrepancy is caused by using the non-boundary conforming approach. In the case of moving structures this approach produces high-frequency oscillations of the lift and drag coefficients primarily because the mesh nodes change their type (i.e. a mesh node falls either into solid region or fluid region) from time step to time step. To reduce these unphysical oscillations the FFT smoothing is used.

A good agreement between numerical and Anderson experimental results is corroborated by Figure 5-*a,b* where measured and predicted mean thrust and power coefficients are shown.

The mean thrust coefficient is expressed as $C_T = \dfrac{2}{T} \displaystyle\int_0^T F_x(t)\, dt$ and the mean input power as

$$C_{ip} = \frac{2}{T}\left[\int_0^T F_y(t)\frac{dh(t)}{dt}\,dt + \int_0^T M(t)\frac{d\theta(t)}{dt}\,dt\right].$$
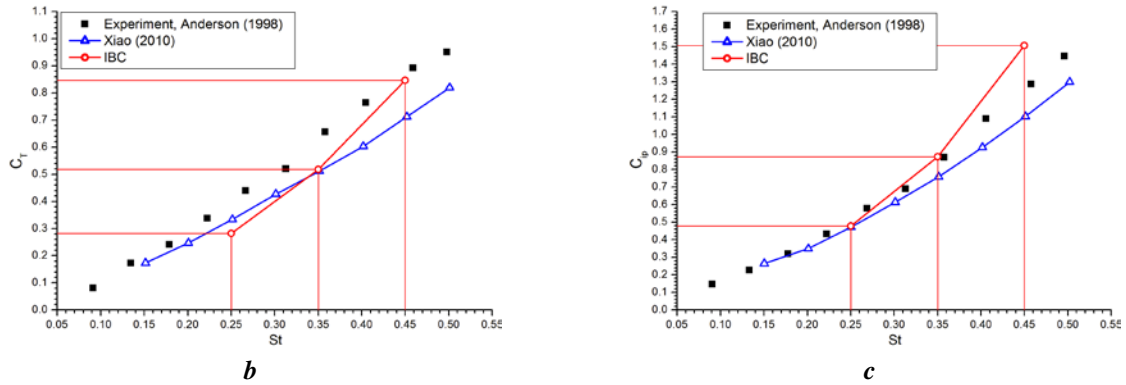
Figure 5: Pitching and plunging NACA0012 foil. (a) Mean trust coefficient. (b) Mean power coefficient.

12 CONCLUSIONS

The paper presents a method for the numerical simulation of fluid-structure interaction using non-boundary conforming unstructured meshes. The mathematical model is based on the compressible Navier-Stokes equations and exploits the Brinkman penalization technique to mimic the influence of structure on a flow. The presence of moving structures is controlled by the time-dependent force term in the governing equations and does not complicate the existing computational algorithm that is based on the higher-accuracy EBR schemes.

In order to illustrate the efficiency of the proposed method, three two-dimensional cases with increasing complexity are considered. All the cases are well documented with a great number of available experimental data and numerical results. The first two cases consider the cylinder oscillations at Re=100 caused either by external or vortex-induced forces. In the third case the pitching and plunging motion of NACA0012 foil at Re=40000 is simulated.

It should be noted that the usage of the immersed boundary methods for moving obstacles requires highly refined meshes in the regions of possible motion trajectories, in order to provide the required (or, at least, acceptable) mesh resolution in the boundary layers formed around the streamlined bodies. This is a weakness of the method. However it can be overcome by the dynamic mesh adaptation. Moreover, the immersed boundary approach allows to operate in simply connected domains which opens a possibility to use efficiently adaptive moving mesh methods. It is a direction of current and future work.

The usage of unstructured meshes, while complicating the numerical algorithm, lets us handle complex geometries and provides wider options for adaptive mesh technologies which is of crucial importance for simulating flow over moving bodies.

13 ACKNOWLEDGMENTS

REFERENCES

[1] Zakaria, M.Y., Pereira, D.A., Ragab, S.A., Hajj, M.R. and Marques F.D. An Experimental Study of Added Mass on a Plunging Airfoil Oscillating with High Frequencies at High Angles of Attack. *33rd AIAA Applied Aerodynamics Conference* (2015), AIAA 2015-3166.

[2] Shiels, D., Leonard, A. and Roshko, A. Flow-induced vibration of a circular cylinder at limiting structural parameters. *Journal of Fluids and Structures* (2001) **15**:3-21.

[3] Li, L., S.J. Sherwin, and P.W. Bearman. "A moving frame of reference algorithm for fluid/structure interaction of rotating and translating bodies. *Int. J. Numer. Meth. Fluids* (2002) **38**:187-206.

[4] Newman, D.J. and Karniadakis, G.E. A direct numerical simulation study of flow past a freely vibrating cable. *J. Fluid Mech.* (1997) **344**:95-136.

[5] Peskin, C.S. Flow patterns around heart valves: a numerical method. *J. Comput. Phys.* (1972) **10**:252-271.

[6] Mittal, R. and Iaccarino, G. Immersed boundary Methods. *Annu. Rev. Fluid Mech.* (2005)

37:239-261.

[7] Angot, Ph., Bruneau, C-H. And Fabrie, P. A penalization method to take into account obstacles in incompressible viscous flows. *Numer. Math.* (1999) **81**:497-520.

[8] Kevlahan, N. K.-R. and Ghidaglia, J.-M. Computation of turbulent flow past an array of cylinders using a spectral method with Brinkman penalization. *Eur. J. Mech.* (2001) **B 20**: 333-350.

[9] Angot, Ph. Analysis of singular perturbations on the Brinkman problem for fictitious domain models of viscous flows. Math. Methods Appl. Sci. (1999) **22**:1395-1412.

[10] Boiron, O., Chiavassa, G. and Donat, R. A high-resolution penalization method for large Mach number flows in the presence of obstacles. *Comput. Fluids* (2009) **38**:703-714.

[11] Liu, Q. and Vasilyev, O.V. Nonreflecting boundary conditions based on nonlinear multidimensional characteristics. *Int. J. Numer. Meth. Fluids* (2010), **62**:24-55.

[12] Abalakin, I.V., Bakhvalov, P.A., Gorobets, A.V., Duben, A.P. and Kozubskaya,T.K. Parallel research code NOISEtte for large-scale CFD and CAA simulations. *Vychisl. Metody Programm.* (2012) **13**(3):110-125, (in Russian).

[13] Abalakin, I., Bakhvalov,P. and Kozubskaya, T. Edge-based reconstruction schemes for unstructured tetrahedral meshes. *Int. J. Numer. Meth. Fluids* (2016) **81**: 331-356.

[14] Abalakin, I., Bakhvalov, P. and Kozubskaya, T. Edge-based reconstruction schemes for prediction of near field flow region in complex aeroacoustic problems. International Journal of Aeroacoustics (2014) 13:207-234.

[15] Bakhvalov, P. and Kozubskaya, T. EBR-WENO scheme for solving gas dynamics problems with discontinuities on unstructured meshes. *Comput.Fluids*(2017) **157**:312-324.

[16] Morison, J. R., et al. The Force Exerted by Surface Waves on Piles. *AIME Petroleum Transactions* (1950) **189**:149-154.

[17] Blevins, R.D. Flow-Induced Vibration, Second edition. Krieger Publishing Company, (2001).

[18] Dütsch, H, Durst, F., Becker, S. and Lienhart, H. Low-Reynolds-number flow around an oscillating cylinder at low Keulegan-Carpenter numbers. *J. Fluid Mech.* (1998) **360**: 249-271.

[19] Vasilyev, O.V. and Kevlahan, N.K.R. An adaptive multilevel wavelet collocation method for elliptic problems. *J. Comput. Phys.* (2005) **206**:412-431.

[20] Anderson, J.M., Streitlien, K., Barrett, D.S. and Triantafyllou, M. S. Oscillating foils of high propulsive efficiency. *J. Fluid Mech.* (1998) **360**:41-72.

[21] Xiao, Q and Liao, W. Numerical investigation of angle of attack profile on propulsion performance of an oscillating foil. *Comput. Fluids* (2010) **39**:1366-1380.